LAWRENCE
LIVERMORE
NATIONAL
LABORATORY

UCRL-JRNL-229297

Templated Control of Au nanospheres in Silica Nanowires

J. W. Tringe, G. Vanamu, S. H. Zaidi

March 22, 2007

Journal of Applied Physics

Disclaimer

Templated control of Au nanospheres in silica nanowires

Joseph W. Tringe

Lawrence Livermore National Laboratory, 7000 East Ave., Livermore, CA, 94551, USA

Ganesh Vanamu

Intel Corporation, 2200 Mission College Blvd, Santa Clara, CA, 95054, USA

Saleem H. Zaidi

Gratings, Inc., 2700 Broadbent Parkway NE, Albuquerque, NM, 87107, USA

The formation of regularly-spaced metal nanostructures in selectively-placed insulating nanowires is an important step toward realization of a wide range of nano-scale electronic and opto-electronic devices. Here we report templated synthesis of Au nanospheres embedded in silica nanowires, with nanospheres consistently spaced with a period equal to three times their diameter. Under appropriate conditions, nanowires form exclusively on Si nanostructures because of enhanced local oxidation and reduced melting temperatures relative to templates with larger dimensions. We explain the spacing of the nanospheres with a general model based on a vapor-liquid-solid mechanism, in which an Au/Si alloy dendrite remains liquid in the nanotube until a critical Si concentration is achieved locally by silicon oxide-generated nanowire growth. Additional Si oxidation then locally reduces the surface energy of the Au-rich alloy by creating a new surface with minimum area inside of the nanotube. The isolated liquid domain subsequently evolves to become an Au nanosphere, and the process is repeated.

I. Introduction

Control of nanoparticle size and spacing is highly desirable for optical, biological, chemical, and electronics applications. For example, by defining the size and shapes of metal nanoparticles, photodetectors and color filters[1-3], substrates for surface enhanced Raman scattering[4-7], surface plasmon devices[8-10], chemical sensors[11-13], and luminescent devices[14] have been realized. Similarly, synthesis of metallic nanoparticles in an insulating matrix has added to the functionality of optical switches and memory devices. Recently, for example, a laser-annealing process in Au_2O-doped glass was used to form an optical diffraction grating[15], and important properties of Au nanospheres in silica nanowires were demonstrated for a wavelength-controlled optical nanoswitch.[16] Semiconductor and metallic nanoparticles integrated into the gate of a field effect semiconductor device have enabled reductions in power consumption and read/write/erase time by acting as discrete charge storage elements.[17-21] Room-temperature single electron devices can also be achieved when charges can be localized in domains a few nm in diameter.[22,23]

Simultaneous control of particle size and spacing is especially useful. For example, building electronic memory elements from nanoparticles requires them to be precisely addressable. Photonic devices can be created with nanowires[24] and regularly-spaced metallic nanoparticles.[25] However, the control necessary to produce such structures has proved elusive at nanometer dimensions with bottom-up processes, and the density of arrays produced by top-down processes such as optical lithography is limited by the wavelength of light used to expose photoresist, or by properties of the photoresist itself. Chemical sensing applications also require control of both particle size and separation. In

the case of metal nanoparticles, these parameters can be tuned to influence surface plasmon resonance effects[26], but in general nanometer-scale control of particle properties remains exceedingly difficult to achieve in practice.

Here we report a process for synthesis of gold (Au) nanospheres embedded in silica nanowires in which control over particle size and spacing is achieved by a self-assembly process initiated at a nanostructured substrate template. Similar Au sphere in silica structures have been previously observed[16,27-29] and with microwave synthesis methods, "pea-pod" structures have been demonstrated with other metals and insulators.[16] Under ultra-high vacuum conditions, Au migration on Si nanowires was observed to play an important role in the growth and resulting structure of the nanowire.[30] However, in oxidizing environments the thermodynamic formation mechanisms can be quite different, as evidenced by the appearance of regularly-spaced Au nanospheres presented here and elsewhere. With the general synthesis model and templated growth advances reported here, the nanowire-embedded spheres provide a powerful bridge between lithographically-defined structures and much smaller self-assembled functional units.

II. Synthesis and properties of nanosphere-embedded nanowires

Au nanospheres were synthesized with a catalyst of Au/Si nanostructures. The fabrication process consists of three steps: (a) formation of nanostructured Si surfaces[31], (b) deposition of 5-100 nm thick Au films by evaporation, and (c) furnace annealing in air for 30-minutes at ~ 1000 °C. Nanostructured Si surfaces described in this work are randomly

patterned, but nanowires may be formed on nanostructured silicon created via non-random processes as well.[32]

Randomly distributed structures with nano- and micrometer scale dimensions in crystalline Si substrates were fabricated using metal-coated films as catalysts in a Plasma-therm parallel plate reactor.[33] The plasma chemistry was based on SF_6 and O_2; flow rates were 14 sccm and 8 sccm, respectively, and the chamber pressure was 170 mTorr with RF power of 300 W. Thin Au films in 5-100-nm thickness range were deposited on Si surfaces by e-beam evaporation. All Si samples with as-deposited Au films were annealed in air in a furnace at 1000° C for 30 minutes. While nanowire synthesis was observed in all cases, the best results were seen for nominal 25-nm Au film thickness.

Scanning electron microscope (SEM) analysis was performed with a Hitachi S-800 field emission system. Samples were mounted on a 45º holder to enable near-90º cross-sectional views of surface features. Transmission electron microscope (TEM) analysis was carried out in a JEOL 2010F field emission STEM/TEM in regular TEM mode, with an accelerating voltage of 200 kV. The TEM sample was prepared by mechanically harvesting the nanowires from the Si substrate, then transferring them to 3 mm holey carbon-coated grid. Photoluminescence (PL) measurements were carried out at room temperature using both 350 nm and 400 nm excitation sources with comparable response.

The SEM image in Figure 1(a) shows as-deposited Au films. Figure 1(b) shows the same surface after high-temperature annealing. This final step results in synthesis of Au nanospheres embedded in silica nanowires. Wires are typically 2-3 μm long, with diameters

between ~10 and 35 nm for nanospheres with diameters ranging between ~5 and ~30 nm. Nanowires of varying diameters form under identical processing conditions, indicating the diameter of the wires are controlled by the properties of the catalyst and substrate. As a control, Au films were simultaneously deposited on microstructured Si surfaces as shown in Fig. 1(c) and (d). Critically, we find that on these larger structures, there was no nanowire growth. Instead, Au films agglomerated into larger islands.

Fig. 2 provides detailed SEM and transmission electron microscope (TEM) views of Au/silica nanowires. The SEM image in Fig. 2(a) shows the orientation of the nanowires relative to the surface and one another. TEM images in Fig. 2(b) and (c) show ~ 5-nm diameter and ~ 24-nm Au spheres embedded in silica nanowires, each separated from its nearest neighbour with a period equal to three times its diameter, as indicated by red circles. Energy dispersive x-ray spectroscopy (EDXS) confirmed that Au was in the nanospheres, and not in the surrounding wires. High-resolution TEM images of the spheres indicated that they were composed of Au, not Au silicide. Silicon and oxygen EDXS contrast levels were consistent with a 1:2 Si:O stoichiometry.

This relative inter-sphere spacing was the same for the large majority of synthesized nanowires. Figs 2(d) and 2(e) are TEM images of a pair of representative wires, where sphere spacing is highlighted with circles in the magnified 2(e). Wires were mechanically harvested from the wafer, so those shown do not necessarily represent a single growth area. Other TEM images of wires harvested from elsewhere on this wafer and other like-processed wafers appeared similar. Although the sphere growth period is not always

exactly three times the average sphere diameter (see for example, the spheres indicated by the arrow in 2(e)), the average spacing for all the spheres shown in Fig. 2 (e) and (f) is within 10% of this value.

Many process conditions were explored for this work, and the roles of Si template geometry, Au thickness and temperature were all examined. Hundreds of nanowires were observed by transmission electron microscopy, and many thousands by scanning electron microscopy. When nanostructured Si features (~100 nm or smaller) are present beneath thin, discontinuous Au films, well-spaced Au nanospheres embedded in silica nanowires result from annealing in air at temperatures 1000º and higher. We have observed the highest density of wires containing Au nanospheres in samples having Si columns with diameters less than 100 nm, covered by 25 nm Au. Au thickness was measured on a simultaneously-deposited planar surface.

Nanowires emit a low-intensity but distinct photoluminescence (PL) band peaking near 440 nm when excited by light at 350 nm as shown in Fig. 3. A similar signal has been observed in much smaller Au_8 nanodots under 366 nm irradiation (emission peak at 450 nm)[14], but also with cathodoluminescence of silica nanowires containing Au nanospheres, where a room-temperature peak near 440 nm was attributed to strain bonds between silicon and oxygen.[16]

III. Formation of silica nanowires on Si nanostructures

To understand how nanospheres form, we first estimate the quantity of Au distributed in silica nanowires. We assume that the nanowires can be modelled simply as embedded Au spheres in a cylinder of silica. A repeating wire segment can be described as a gold sphere inside of a silica right cylinder with radius R_{silica}, where the cylinder has a total length of six times the Au sphere radius, R_{Au}. The volume fraction of Au, V_{Au}/V_{silica}, can then be estimated as:

$$\frac{V_{Au}}{V_{silica}} = \frac{\frac{4}{3}\pi R_{Au}^3}{(\pi R_{silica}^2)\times 6R_{Au} - \frac{4}{3}\pi R_{Au}^3} \qquad (1)$$

Although there can be some variation in wire radius, experimentally we find (1) reduces to 5-10% for all observed wires. Very similar ratios have been observed by others[16,28,29] for Au nanospheres in silica nanowires formed by widely divergent processes.

For 2000-nm length wires with 5 and 24 nm spheres, the Au/Si volume ratio implies Au precursor islands with diameters of ~17 and 36 nm, respectively. This is consistent with previous observations of planar surfaces where nanoscale Au islands of similar dimensions are formed from semi-continuous thin films at low annealing temperatures. For example, Au islands have been observed to form from a ~10 nm thick Au film on planar Si heated to 200 °C for ~10 minutes.[34] Also, Au nanoparticles have been shown to develop in just 30 minutes in a Si/Au system at 250 °C.[35]

The size of the Au islands is similar on the Si micro- and nano-structured substrates since both had comparable amounts of Au deposited on their surfaces. Why then do the nanowires form exclusively on nanostructured substrates? We hypothesize nanowire formation is favoured when the nanostructured Si is near its melting temperatures. Since the bulk melting temperature of Si is 1414 °C, the melting temperature of Si must be significantly reduced for nanowire formation to proceed at 1000 °C. In fact, such melting point lowering has been observed: Si islands on silica that are between 80 and 300 nm wide have been melted at ~1110 ºC.[36] Since our Si nanostructured features have typical radii of less than 100 nm, these will be significantly relaxed, if not melted, at 1000 °C, enough to allow efficient diffusion of Si into Au, thus initiating the nanowire formation process.

We propose that silicon oxide nanowires form on Si nanostructures by a vapor-liquid-solid (VLS) process, with oxygen as the primary species provided in the gas phase for nanowire growth. Oxide growth is tremendously accelerated in the presence of Au because the Au/Si alloy is much more efficient at delivering Si for oxide growth relative to a solid Si surface. This is well-known, for example, from oxidation studies for Si on planar surfaces. A temperature of ~ 1100 °C is required to form a 100-nm thick oxide layer on Si in 20 minutes. However, for an Au/Si surface, the same thickness oxide film can be grown at only ~ 250 °C in air in comparable time.[37]

We propose that silica nanowires form as shown in Fig. 4(a). First, Au islands develop on nanostructured Si substrates as previously described, and the enhanced rate of

Si oxidation at the edges of Au islands pushes the Au island above the surface of the Si. As annealing continues for longer durations and higher temperatures, more Si diffuses through the central channel into the Au reservoir in quantities sufficient to sustain subsequent nanowire growth. For example, assuming 1:2 Si:O stoichiometry in the nanowire, and all Si provided by the substrate, the Au/Si reservoir diameters would initially be ~50 and 90 nm for nanowires with 5 and 24-nm diameter Au nanospheres, respectively, just prior to nanowire initiation. A significant quantity of Si must originate from the substrate; otherwise nanowires would form on microstructured Si surfaces. However, since we cannot exclude the possibility that some Si is provided by the vapor phase, these reservoir diameters represent upper bounds. Wire diameters are determined by the size of the Au/Si reservoir, with larger-diameter wires created by larger-diameter reservoirs.

Next, nanowires grow from the reservoir. At a temperature of ~ 1000 °C the Au/Si alloy reservoir must be liquid to facilitate nanowire formation. Silica growth at the base of the liquid Au/Si alloy reservoir forms a rigid cylinder, which then extends away from the substrate. As oxide formation proceeds, Au segregates on the Si side of the Si/silica interface since Au is much less soluble in silica vs. Si .[38] Oxide actually forms all around the reservoir, but growth is fastest at the base because as the wire is formed fresh Si/Au alloy is exposed directly to the oxygen-rich ambient. Evidence for the reservoir has been provided TEM images shown in Fig. 4(b), (c) and elsewhere.[16,29]

According to the Si/Au equilibrium phase diagram, a maximum of ~15% Si by weight is soluble in Au at 1000 °C. However, the nanowire growth system differs from the

ideal bulk equilibrium system. In particular, we observe that in Au/silica nanowires (irrespective of nanosphere radius), the final weight composition is 40-50% Si. This is further evidence that the melting temperature of Au/Si nanostructures is depressed relative to its bulk equilibrium value, though it is possible some additional Si is being supplied in the vapor phase from the substrate. This is vapor liquid solid (VLS) growth because of the presence of the liquid reservoir on top of the nanowire; here the reservoir is consumed during nanowire growth and therefore does not act purely as a catalyst. Unlike size selection by metal-induced crystallization or amorphization which results in 1-2 nm particles,[35] this mechanism relies on metal-induced oxidation, with the resulting nanosphere size being set by a combination of the thermodynamically-controlled oxidation rate and the Si/Au ratio.

IV. Formation of Au nanospheres in silica nanowires

We have now identified mechanisms for nanowire formation exclusively on Si nanostructures, but have not described how Au nanospheres are created. We hypothesize a nanosphere formation process similar to that first suggested by Wu et al.[27], but initiated sequentially near the reservoir by the process illustrated in Fig. 5. Here a Au/Si filled reservoir facilitates growth of the nanowire through rapid oxidation at the interface between the reservoir and the nanowire, forming a cylindrical oxide shell around a liquid Au/Si dendrite. The high local curvature of the tip of the dendrite depresses the dendrite melting temperature relative to the reservoir melting temperature according to:

$$T(H) = T(H = 0) - \frac{2\gamma V^S}{\Delta S} H \quad (2)$$

where γ is the surface energy of the liquid-solid interface, V^S is the molar volume of the solid, and ΔS is $S^L - S^S$, the entropy of fusion.[39] H is the curvature, defined as:

$$H = \frac{1}{2}\left(\frac{1}{r_1} + \frac{1}{r_2}\right). \quad (3)$$

r_1 and r_2 are radii of curvature along orthogonal axes defined on a two-dimensional surface such as a section of a sphere (for the reservoir, or tip of the dendrite) or cylinder (for the nanowire). The curvature for a nanowire with 24-nm diameter Au nanospheres is shown in Fig. 5(a), where r_1 is the radius of the reservoir and r_2 is the radius of the nanosphere and tip of the dendrite.

We propose that the Si content at the tip of the dendrite is also depressed relative to the reservoir, implying a concentration gradient is maintained in the dendrite. Si concentration is reduced preferentially in the dendrite because of the rapid Si oxidation that proceeds all around the dendrite during nanowire growth. The higher surface-to-volume ratio of the cylindrical nanowire allows the oxidation of Si in the dendrite to proceed more rapidly compared to oxidation of Si in the reservoir. The existence of a Si concentration gradient in the reservoir and dendrite during nanowire growth is supported by the presence of Au in the final nanowire structure. If, for example, Si in the reservoir could diffuse instantaneously to the growth surface immediately below the reservoir, then the nanowire

would be solid silicon oxide and the Au in the reservoir would act exclusively as a catalyst. Under some substrate-initiated nanowire growth conditions solid Si oxide wires are observed, as are extended Au dendritic structures. These structures indicate that the formation of regularly-spaced nanospheres occurs only under specific conditions.

During the formation of regularly-spaced Au nanospheres, we propose that the concentration of Si is in the dendrite can be modelled as linear function of the distance, z′, from the point when the reservoir begins to taper to closing end of the dendrite:

$$x_{Si}(z') = x_{Si}^{0} - mz' \qquad (4)$$

As shown in Fig. 5(a), the length of the taper can be taken to be proportionate to the radius of the dendrite, r_2. For illustration we assume the length of the taper is equal to $2r_2$. In Eq. 4, x_{Si}^{0} is the concentration of Si in the reservoir, which we take to be between 40-50 weight percent Si based on Au/Si in the final nanowire structure (and assuming relatively little Si is provided from the vapour phase). In this model, m, the slope of the concentration gradient, is proportional to l because the wire's greater surface-to-volume ratio relative to the spherical reservoir induces faster oxidation of Si in the nanowire. The slope m is inversely proportional to the cross-sectional area of the dendrite since the relative amount of Si consumed is proportional to the amount of Si present in the dendrite at the beginning of the process. Taken together these two assumptions imply,

$$m = \frac{cl}{\pi r_2^2} \tag{5}$$

where c is a unitless constant. The value of c has not been experimentally determined, and so the value for m shown in Fig. 5(a) is for illustration only. Note, however, that the Si concentration in the reservoir remains constant during growth as both Si and Au are removed at rates which are proportionate to their respective concentrations in the reservoir at the time when nanowire growth is initiated from the Si surface. Also, we assume the slope is independent of the nanowire growth velocity, though there is likely a threshold velocity corresponding to a minimum oxygen concentration in the growth ambient below which Au nanosphere formation will not proceed. This threshold effect has recently been reported by Kolb et al., for example.[29]

Now the surface energy of the Au/Si alloy in the dendrite is a function of the Si concentration, since the surface tension of pure Au is significantly higher than the surface energy of Si: 1140×10^{-3} vs. 730×10^{-3} J/m^2 at their respective melting temperatures.[39] This implies that there is a critical concentration x_{Si}^{crit}, defined at the growth surface of the nanowire ($z' = 2r_2$) at which reduction of dendrite surface/volume ratio becomes energetically favoured compared with cylindrical extension of the dendrite. Reduction of the dendrite surface/volume ratio may occur through the formation of a section of a spherical (or more curved) surface at the oxide/dendrite interface, while cylindrical extension of the nanowire is equivalent to maintaining a constant surface-to-volume ratio in the dendrite. This is an unstable equilibrium process: oxidation which locally minimizes

the surface area (by beginning the formation of the hemispherical cap) also removes Si, further increasing the energetic driving force per area. The important role of oxidation for sphere formation is consistent with the findings of Kolb et al.[29], who demonstrate that the operation of the sphere formation mechanism is sensitive to the amount of oxygen present in the growth ambient. Note that some nanowire growth conditions allow extended Au dendrites to persist many nanowire radii away from the reservoir; in this case the unstable equilibrium caused by the dependence of the dendrite surface energy on Si concentration may still allow the formation of Au nanospheres, though inter-sphere spacing may be less regular.

For formation of regularly-space spheres, there is a dendrite length $l = L_{crit}$ when the critical Si concentration x_{Si}^{crit} is realized at the edge of the growth surface ($z' = 2r_2$). From Eqs. 4 and 5:

$$x_{Si}^{crit}(z' = 2r_2) = x_{Si}^{0} - \left(cL_{crit} \times 2r_2 \Big/ \pi r_2^2 \right) \tag{6}$$

Experimentally, we observe that $L_{crit} = \sim 6r_2$, so that (6) reduces to:

$$x_{Si}^{crit}(z' = 2r_2) = x_{Si}^{0} - 12c/\pi \tag{7}$$

This value is independent of nanowire geometry and substrate conditions, in agreement with our experimental results. The process independence of this result explains the

remarkable geometrical consistency of the Au "pea-pod" structures observed by several recent workers for a wide range of growth conditions.[16,27-29]

Once the Au/Si alloy in has been isolated from the reservoir by oxidation by the formation of a highly-curved, low surface-to-volume ratio oxide cap as described above, then the isolated volume continues to evolve to become a Au sphere, as illustrated in Fig. 5(b). The driving force continues to be the reduction of surface energy. The evolution proceeds from the more curved ends of the isolated volume to the center because, relative to the center, the ends are both lower in Si (and therefore higher in surface energy) and more mobile since the locally higher curvature depresses the melting temperature.

It is notable that nanospheres with diameters significantly above ~30 nm have not been observed. This is likely due to the requirement that the Au/Si alloy remain liquid in the dendrite and nanowire for sphere formation to proceed, and that this condition can be met only with curvature-induced melting temperature lowering (Eq. 2). For nanowires with internal radii significantly larger than ~30 nm, this melting temperature lowering is insufficient for sphere formation to proceed.

Some larger-diameter silica nanowires form without embedded Au spheres, as shown in Fig. 4(c). Especially at the ends of silica wires, we find some malformed spheres and extended internal Au structures (Fig. 4(b) and Fig. 4(c) indicated by arrows). We attribute these features to exhaustion of Si in the Au/Si reservoir, which prevents the formation of Au/Si dendrites. Sphere periods smaller or larger than three sphere diameters (for example,

shown in Fig. 2(e)) may be due to the interaction of growing wires with other wires or with the nanostructured Si substrate, which would temporarily distort the growth geometry or locally alter the stoichiometry.

A similar spacing may be predicted under certain conditions by processes related to a Rayleigh instability,[29] which is driven by surface energy minimization. The canonical Rayleigh instability, however, does not account for surface energy changes due to compositional differences, nor for the effect of a new solid matrix surrounding the disintegrating liquid stream. During Au nanosphere formation Si must segregate from the liquid Au/Si alloy, at which time it immediately solidifies into silica in the oxidizing environment - or else remains as crystalline Si if insufficient oxygen is available.[29] For comparison, in the GaN system, Ga-filled GaN nanotubes have been synthesized using an Au catalyst in a nitrogen ambient. Here, however, the very low melting temperature of Ga (30 °C, vs.1064 °C for Au) allowed the entire tube to be filled with liquid Ga during growth.[40]

Wu et al. [27] and Hu et al.[16] have presented qualitative models and evidence for Au nanosphere formation in silica nanowires. Wu et al. first envisioned nanospheres developing by a two-stage process in which a cylindrical Au silicide core is first embedded in a Si nanotube, which subsequently oxidizes. More recently, Hu et al.[16] provide TEM evidence of a proposed nanowire growth mechanism in which a Au/Si alloy forms an extended tube which subsequently evolves to distinct nanospheres. This growth mode may be possible under their process conditions since Si is being injected from the plasma

ambient to maintain a constant concentration in the liquid Au/Si alloy during nearly the entire growth period of the nanowire. As the nanowire oxide sidewall thickness increases (or the plasma is turned off), less Si penetrates the cylindrical oxide shell, and nanosphere formation may proceed simultaneously from multiple nucleation sites throughout the length of the wire.

In summary, our proposed model for nanosphere formation provides that the higher surface-to-volume ratio in the nanowire enables a Si gradient to exist in a Si/Au dendrite extending from the reservoir, while atomic mobility is increased by curvature-induced melting temperature lowering. Because of the higher surface energy of Au vs. Si, the surface energy of the Au/Si alloy increases at the growth surface when the Si concentration is locally reduced in the dendrite through oxidation. When the dendrite reaches a length corresponding to a (Au-rich) critical Au/Si ratio, then the dendrite is isolated from the reservoir by a curved oxide cap which locally reduces the surface energy by minimizing the surface/volume ratio. This isolated Au/Si volume subsequently evolves to a sphere, consuming the remaining Si by oxidation and minimizing the surface energy of the Au that remains. Simultaneously, nanowire growth and dendrite extension proceed at the base of the reservoir, periodically repeating the nanosphere formation process.

V. Summary

We have demonstrated controlled synthesis of Au nanospheres in silica nanowires, where spheres are periodically spaced with a period equal to three sphere diameters. Nanowires

are created only on nanostructured Si templates, and not on larger structures. We explain this selective growth phenomena and the sphere formation process thermodynamically with melting temperatures in Si nanostructures that are depressed relative to micron-scale structures, and by Si oxidation that is accelerated in the presence of Au. Au islands formed on Si nanostructures evolve into nanometer-scale reservoirs of liquid Si/Au that are subsequently lifted off the Si substrate by oxidation. These reservoirs facilitate Au nanosphere formation through a two-step process which includes rapid formation of a silica nanotube followed by precipitation of Si from the Au/Si alloy in local domains of lower Si concentration and higher curvature inside the nanotube. The thermodynamic understanding of sphere formation and its controlled synthesis can allow accelerated realization of devices such as plasmonic waveguides and single-electron memories.

Acknowledgements

We are grateful for illuminating and productive discussions with Dr. Harold Levie at Lawrence Livermore National Laboratory, Dr. Albert Davydov at the National Institute of Standards and Technology, Prof. L.-C. Chen at the National Taiwan University, Prof. K.-H. Chen at the National Taiwan University and Academia Sinica, Prof. Nadya Mason at the University of Illinois Urbana-Champaign, and Dr. Charles Stevens at Lawrence Livermore National Laboratory. We thank Dr. Carolyn Matzke for photoluminescence measurements, Rajiv Prinja for Au depositions, and Richard Marquardt for processing support. We also thank Prof. Abhaya Datye and Ying Bing of the University of New Mexico for TEM support. One of the authors (SHZ) acknowledges partial support by the US Department of Defense under contract # FA9453-05-C-0058. This work was performed under the auspices of the US Dept. of Energy by the Univ. of California Lawrence Livermore National Laboratory under Contract W-7405-ENG-48.

Correspondence and requests for material should be sent to J.T. (tringe2@llnl.gov).

Figure captions

Figure 1. (a) Scanning electron microscope image of as-deposited Au film on a nanostructured Si surface, and (b) Au sphere/nanowire formation after annealing. (c) Scanning electron microscope image of as-deposited Au film on a microstructured Si surface , and (d) Au consolidation without nanowire formation after annealing.

Figure 2. (a) Scanning electron microscope image of nanowires and substrate (b) Transmission electron microscope image of nanowires with ~5-nm diameter, and (c) ~ 24-nm diameter. (d) and (e) show longer segments of two nanowires where the average sphere period is within 10% of three sphere diameters. Red circles illustrate that the inter-sphere period is equal to three sphere diameters in most cases, though an exception indicated by an arrow is apparent in (e).

Figure. 3 Photoluminescence from silica nanowires containing Au nanospheres with excitation wavelength 350 nm.

Figure 4. (a) Au/Si reservoir initiation on a Si nanostructure, (b) TEM image of Au reservoir at nanowire termination with Si exhausted. Red circles illustrate that the inter-sphere spacing has a period equal to three sphere diameters. (c) shows many nanowires, including two (indicated by arrows) in which the extended reservoir at nanowire terminus is apparent.

Figure 5. A model for Au nanosphere formation: (a) curvature, surface/volume ratio and weight percent Si as a function of distance from the tip of the nanowire. An isolated Au/Si domain begins to form at the point where the nanowire meets the tapered reservoir when the local Si concentration reaches a critical value. The Si concentration at this location is reduced by oxidation in the extended Au/Si alloy dendrite. Eq. 3-7 describe the thermodynamic driving forces for this process. (b) Au nanosphere definition during nanowire growth. Si in isolated domains of Au/Si alloy is oxidized, reducing the surface area of the remaining domain until a Au sphere is formed.

References

[1] G. Konstantatos, I. Howard, A. Fischer, S. Hoogland, J. Clifford, E. Klem, L. Levina, and E. H. Sargent, Nature **442,** 180-183 (2006).

[2] Y. Dirix, C. Bastiaansen, W. Caseri, and P. Smith, Advanced Materials **11,** 223-+ (1999).

[3] C. L. Haynes and R. P. Van Duyne, Nano Letters **3,** 939-943 (2003).

[4] M. Kahl, E. Voges, S. Kostrewa, C. Viets, and W. Hill, Sensors and Actuators B-Chemical **51,** 285-291 (1998).

[5] K. Kneipp, A. S. Haka, H. Kneipp, K. Badizadegan, N. Yoshizawa, C. Boone, K. E. Shafer-Peltier, J. T. Motz, R. R. Dasari, and M. S. Feld, Applied Spectroscopy **56,** 150-154 (2002).

[6] R. G. Freeman, K. C. Grabar, K. J. Allison, R. M. Bright, J. A. Davis, A. P. Guthrie, M. B. Hommer, M. A. Jackson, P. C. Smith, D. G. Walter, and M. J. Natan, Science **267,** 1629-1632 (1995).

[7] R. G. Freeman, M. B. Hommer, K. C. Grabar, M. A. Jackson, and M. J. Natan, Journal of Physical Chemistry **100,** 718-724 (1996).

[8] S. A. Maier, M. L. Brongersma, P. G. Kik, S. Meltzer, A. A. G. Requicha, and H. A. Atwater, Advanced Materials **13,** 1501-+ (2001).

[9] P. C. Andersen and K. L. Rowlen, Applied Spectroscopy **56,** 124A-135A (2002).

[10] P. Mulvaney, Langmuir **12,** 788-800 (1996).

[11] R. C. Mucic, J. J. Storhoff, C. A. Mirkin, and R. L. Letsinger, Journal of the American Chemical Society **120,** 12674-12675 (1998).

[12] J. C. Riboh, A. J. Haes, A. D. McFarland, C. R. Yonzon, and R. P. Van Duyne, Journal of Physical Chemistry B **107,** 1772-1780 (2003).

[13] J. M. Nam, C. S. Thaxton, and C. A. Mirkin, Science **301,** 1884-1886 (2003).

[14] J. Zheng, J. T. Petty, and R. M. Dickson, Journal of the American Chemical Society **125,** 7780-7781 (2003).

[15] S. L. Qu, J. R. Qiu, C. J. Zhao, X. W. Jiang, H. D. Zeng, C. S. Zhu, and K. Hirao, Applied Physics Letters **84,** 2046-2048 (2004).

[16] M. S. Hu, H. L. Chen, C. H. Shen, L. S. Hong, B. R. Huang, K. H. Chen, and L. C. Chen, Nature Materials **5,** 102-106 (2006).

[17] Y. C. King, T. J. King, and C. M. Hu, Ieee Transactions on Electron Devices **48,** 696-700 (2001).

[18] E. Kapetanakis, P. Normand, D. Tsoukalas, K. Beltsios, J. Stoemenos, S. Zhang, and J. van den Berg, Applied Physics Letters **77,** 3450-3452 (2000).

[19] Z. T. Liu, C. Lee, V. Narayanan, G. Pei, and E. C. Kan, Ieee Transactions on Electron Devices **49,** 1606-1613 (2002).

[20] Z. T. Liu, C. Lee, V. Narayanan, G. Pei, and E. C. Kan, Ieee Transactions on Electron Devices **49,** 1614-1622 (2002).

[21] *Clusters and Colloids*; *Vol.*, edited by G. Schmid (VCH, New York, 1994).

[22] M. H. Devoret and R. J. Schoelkopf, Nature **406,** 1039-1046 (2000).

[23] K. Yano, T. Ishii, T. Hashimoto, T. Kobayashi, F. Murai, and K. Seki, Ieee Transactions on Electron Devices **41,** 1628-1638 (1994).

[24] M. S. Gudiksen, L. J. Lauhon, J. Wang, D. C. Smith, and C. M. Lieber, Nature **415,** 617-620 (2002).
[25] S. A. Maier and H. A. Atwater, Journal of Applied Physics **98,** - (2005).
[26] R. Gupta, M. J. Dyer, and W. A. Weimer, Journal of Applied Physics **92,** 5264-5271 (2002).
[27] J. S. Wu, S. Dhara, C. T. Wu, K. H. Chen, Y. F. Chen, and L. C. Chen, Advanced Materials **14,** 1847-1850 (2002).
[28] M. Paulose, C. K. Varghese, and C. A. Grimes, Journal of Nanoscience and Nanotechnology **3,** 341-346 (2003).
[29] F. M. Kolb, A. Berger, H. Hofmeister, E. Pippel, U. Gosele, and M. Zacharias, Applied Physics Letters **89,** - (2006).
[30] J. B. Hannon, S. Kodambaka, F. M. Ross, and R. M. Tromp, Nature **440,** 69-71 (2006).
[31] S. H. Zaidi, D. S. Ruby, and J. M. Gee, Ieee Transactions on Electron Devices **48,** 1200-1206 (2001).
[32] A. K. Sharma, S. H. Zaidi, S. Lucero, S. R. J. Brueck, and N. E. Islam, Iee Proceedings-Circuits Devices and Systems **151,** 422-430 (2004).
[33] D. S. Ruby, S. Zaidi, S. Narayanan, S. Yamanaka, and R. Balanga, Journal of Solar Energy Engineering-Transactions of the Asme **127,** 146-149 (2005).
[34] T. F. Young, J. F. Chang, and H. Y. Ueng, Thin Solid Films **322,** 319-322 (1998).
[35] A. Chandra and B. M. Clemens, Journal of Applied Physics **96,** 6776-6781 (2004).
[36] D. Zubia, S. H. Zaidi, S. R. J. Brueck, and S. D. Hersee, Applied Physics Letters **76,** 858-860 (2000).
[37] A. Hiraki, J. W. Mayer, and E. Lugujjo, Journal of Applied Physics **43,** 3643-& (1972).
[38] J. S. Williams, K. T. Short, and A. E. White, Applied Physics Letters **70,** 426-428 (1997).
[39] R. T. DeHoff, *Thermodynamics in Materials Science* (McGraw-Hill, Inc., San Francisco, 1993).
[40] M. C. Lu, Y. L. Chueh, L. J. Chen, L. J. Chou, H. L. Hsiao, and A. B. Yang, Electrochemical and Solid State Letters **8,** G153-G155 (2005).

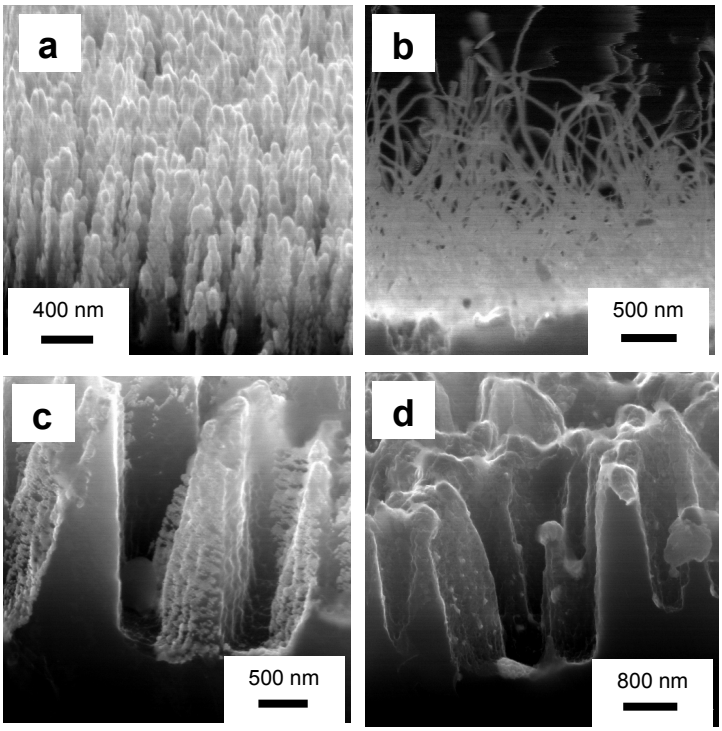

Figure 1.

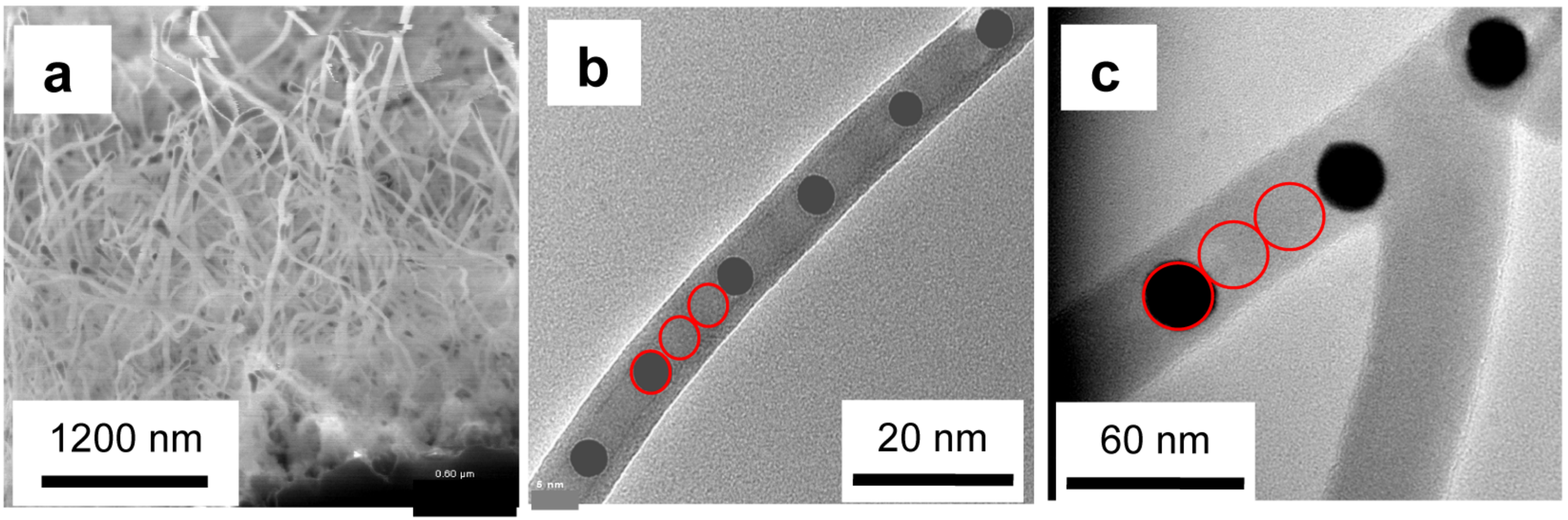

Figure 2.

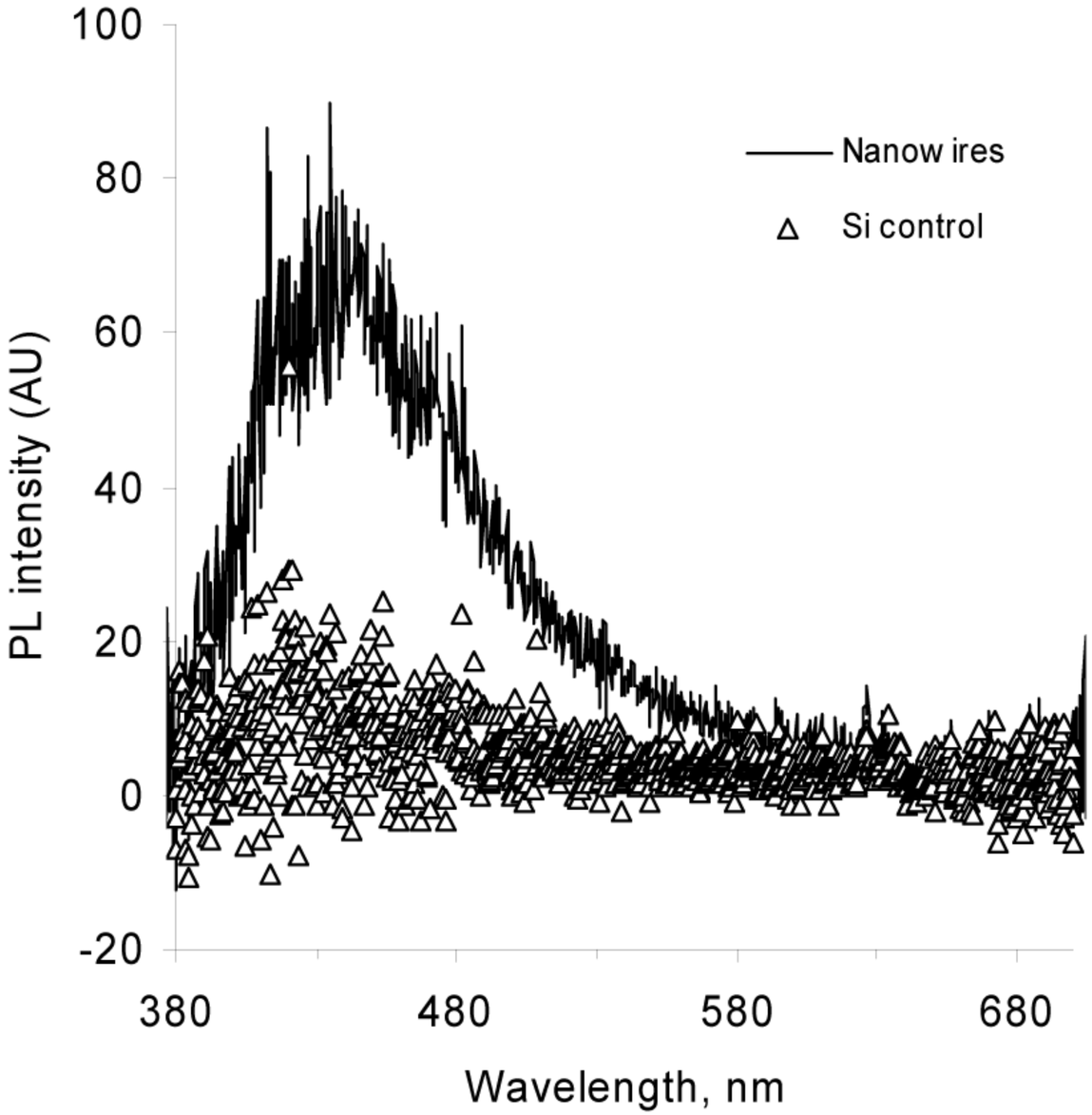
100
80
60
40
20
0
-20
PL intensity (AU)
380
480
580
680
Wavelength, nm
Nanow ires
Si control

Figure. 3

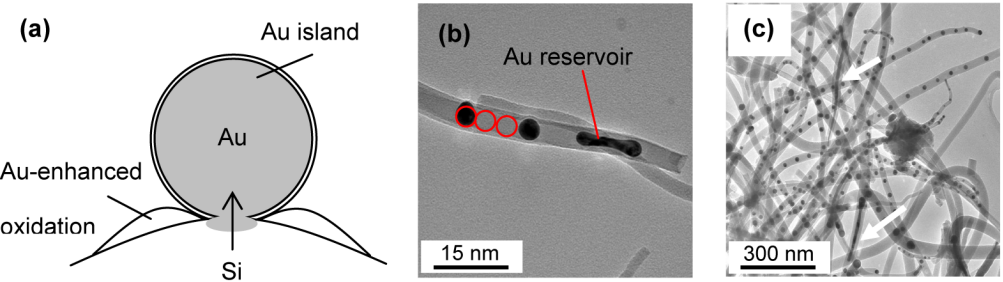
(a)
Au island
Au
Au-enhanced
oxidation
Si
(b)
Au reservoir
15 nm
(c)
300 nm

Figure 4.

(a)

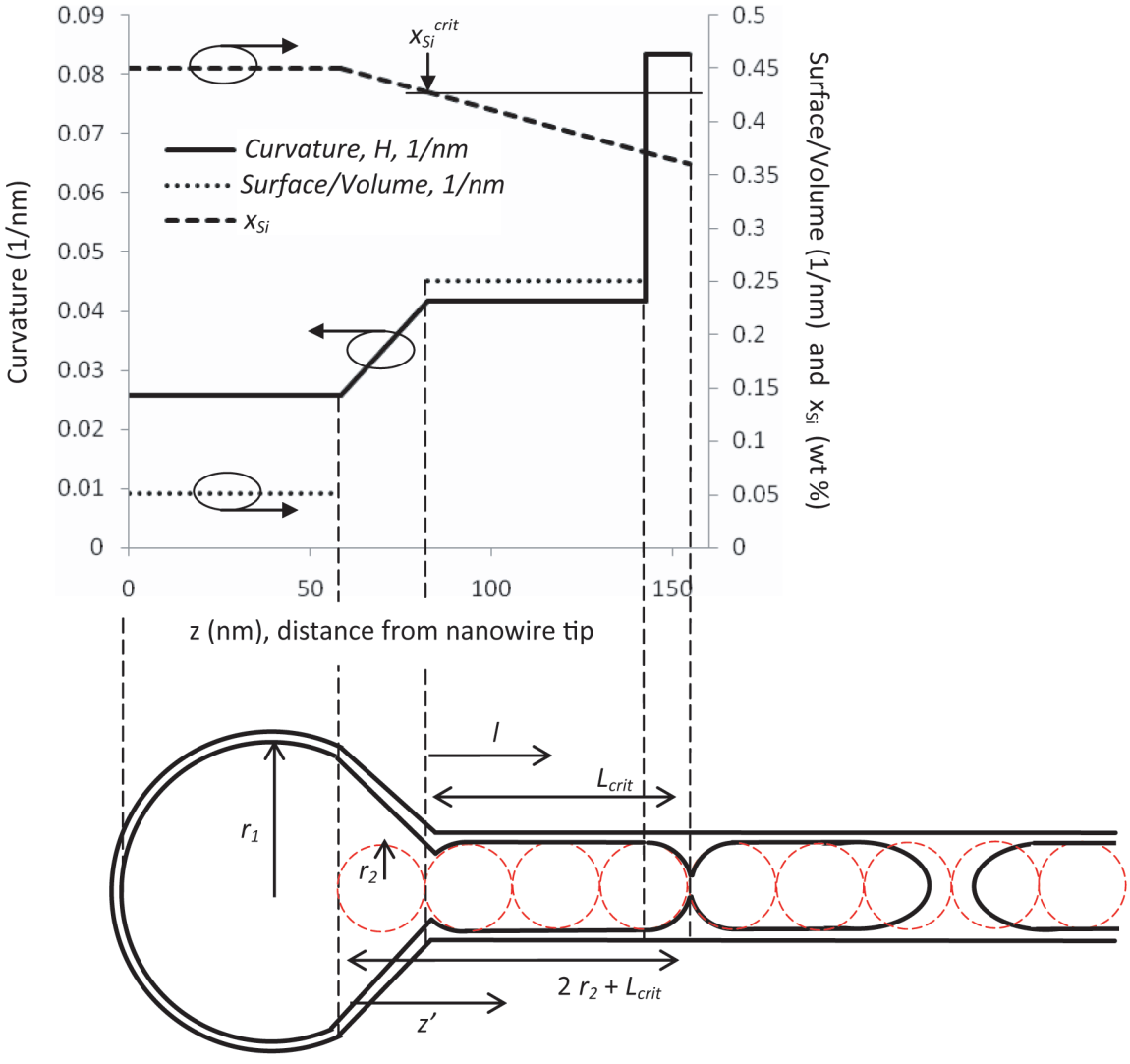
0.09
0.08
0.07
0.06
0.05
0.04
0.03
0.02
0.01
0
0.5
0.45
0.4
0.35
0.3
0.25
0.2
0.15
0.1
0.05
0
x_{Si}^{crit}
Curvature, H, 1/nm
Surface/Volume, 1/nm
x_{Si}
Curvature (1/nm)
Surface/Volume (1/nm) and x_{Si} (wt %)
0
50
100
150
z (nm), distance from nanowire tip
r_1
r_2
l
L_{crit}
$2\ r_2 + L_{crit}$
z'

(b)

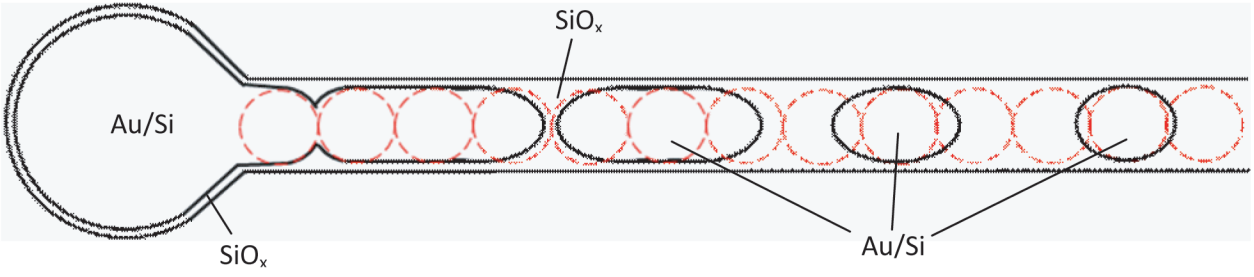
SiO_x
Au/Si
SiO_x
Au/Si